

1 Dear Thorsten Kiefer,

2

3 First of all on behalf of the authors, I would like to thank the reviewers for their
4 invaluable criticism and suggestions. I believe that we have successfully integrated all the
5 reviewers comments and requests, and that these changes have greatly improved the manuscript,
6 as you will be able to appreciate on reading the updated version enclosed here. The additions and
7 changes have been highlighted for convenience.

8 The text has been modified throughout taking into account the reviewers most important
9 comments, regarding: **1. The interpretation and choice of the proxies, in particular the**
10 **elemental ratios; 2. A reevaluation of the climatic phenomena that potentially affected the**
11 **Río de la Plata river discharge.** In addition figure 4 was removed as suggested by the
12 reviewers. We have also responded with an Author Comment to all reviewer comments and
13 suggestions, and have revised and changed the text accordingly.

14 I look forward to hearing from you and should you have any further queries please do not
15 hesitate to contact me.

16 Yours sincerely,

17 Laura Perez

18

19

20

21

22

23

24 **Variability in terrigenous sediment supply offshore of the Rio de la Plata (Uruguay)**
25 **recording the continental climatic history over the past 1200 years**

26

27 L. Perez^{1,4*}, F. García-Rodríguez^{1,4}, T. J. J. Hanebuth^{2,3}

28 ¹ Sección Oceanología, Facultad de Ciencias, Universidad de la República, Iguá 4225,
29 Montevideo 11400 (Uruguay).

30 ² School of Coastal and Marine Systems Sciences, Coastal Carolina University, SC 29528
31 (USA).

32 ³ MARUM – Center for Marine Environmental Sciences, University of Bremen, Leobener
33 Straße, 28359 Bremen (Germany).

34 ⁴ Centro Universitario Regional Este, CURE-Rocha, Ruta 9 intersección Ruta 15, Rocha
35 (Uruguay).

36 Correspondence to: L. Perez (lp3_3@hotmail.com)

37

38

39 **Abstract**

40 The continental shelf adjacent to the Río de la Plata (RdIP) exhibits extremely complex
41 hydrographic and ecological characteristics which are of great socio-economic importance. Since
42 the long-term environmental variations related to the atmospheric (wind fields), hydrologic
43 (freshwater plume), and oceanographic (currents and fronts) regimes are little known, the aim of
44 this study is to reconstruct the changes in the terrigenous input into the inner continental shelf
45 during the Late Holocene period (associated with the RdIP sediment discharge) and to unravel
46 the climatic forcing mechanisms behind them. To achieve this, we retrieved a 10-m long
47 sediment core from the RdIP mud depocenter at 57 m water depth (GeoB 13813-4). The
48 radiocarbon age control indicated an extremely high sedimentation rate of 0,8 cm per year,
49 encompassing the past 1200 years (750-2000 AD). We used element ratios (Ti/Ca, Fe/Ca, Ti/Al,
50 Fe/K) as regional proxies for the fluvial input signal, and the variations in relative abundance of
51 salinity-indicative diatom groups (freshwater versus marine-brackish), to assess the variability in
52 terrigenous freshwater and sediment discharges. Ti/Ca, Fe/Ca, Ti/Al, Fe/K and the freshwater
53 diatom group showed the lowest values between 850 and 1300 AD, while the highest values
54 occurred between 1300 and 1850 AD.

55 The variations in the sedimentary record can be attributed to the Medieval Climatic Anomaly
56 (MCA) and the Little Ice Age (LIA), both of which had a significant impact on rainfall and wind
57 patterns over the region. During the MCA, a northward migration of the Intertropical
58 Convergence Zone (ITCZ), and an associated weakening of the South American Summer
59 Monsoon System (SAMS) and the South Atlantic Convergence Zone (SACZ), could explain the
60 lowest element ratios (indicative of a lower terrigenous input) and a marine-dominated diatom
61 record, both indicative of a reduced RdIP freshwater plume. In contrast during the LIA, the
62 southward migration of the ITCZ, and a strengthening of SAMS and SACZ, may have led to an
63 expansion of the RdIP river plume to the far north, as indicated by higher element ratios and a
64 marked freshwater diatom signal. Furthermore, a possible multi-decadal oscillation probably
65 associated with AMO since 1300 AD, reflects the variability in both the SASM and SACZ
66 systems.

67 **Keywords**

68 Terrigenous sediment supply, element ratios, salinity-indicative diatom groups, historical
69 climatic changes, Intertropical Convergence Zone, South American Summer Monsoon System,
70 South Atlantic Convergence Zone, Río de la Plata, mud depocenter, continental shelf, Uruguay.

71 **1 Introduction**

72 The Río de la Plata (RdIP) estuary is fed by the Paraná and the Uruguay Rivers and drains into
73 the Southwestern Atlantic Ocean (SWAO) forming the second largest estuary system in South
74 America (Bisbal, 1995; Acha et al., 2003). The RdIP is the main source of continental freshwater
75 and sediments entering the SWAO (Piola et al., 2008; Krastel et al., 2011, 2012; Razik et al.,
76 2013; Lantzsch et al., 2014; Nagai et al., 2014). In this sense, the RdIP provides an average
77 annual suspended sediment load of 79.8×10^6 tons yr^{-1} (Depetris et al., 2003). Most of this
78 discharge is directed close to the Uruguayan coast towards the inner continental shelf (Depetris
79 et al., 2003; Gilberto et al., 2004). The RdIP freshwater discharge, leads to a low salinity plume
80 on the inner continental shelf, which can reach northerly areas up to a latitude 28° south (Piola et
81 al. 2000). The low-salinity waters on the inner part of the continental shelf extend downwards to
82 a depth of approximately 50 m, while the outer part of the continental shelf (from 50 m to 200 m)
83 is influenced by the Subtropical Confluence, where the warm, salty southward-flowing Brazil
84 Current collides with the cold and less salty northward-flowing Malvinas Current (Piola et al.,
85 2000).

86 The Paraná River contributes about 73% to the total RdIP freshwater discharge and maximum
87 values are found during austral summer (Depetris and Pasquini, 2007). This precipitation and
88 river discharge pattern is associated with the southward expansion and intensification of the
89 South American Summer Monsoon System (SAMS; Zhou and Lau, 1998; Chiessi et al., 2009).
90 The SAMS is known to be a poleward displacement of the Intertropical Convergence Zone
91 (ITCZ), and is associated with a wet season that begins in the equatorial Amazon and propagates
92 rapidly eastward and southeastward during austral spring (García and Kayano, 2010). The SAMS
93 is tightly associated with the South Atlantic Convergence Zone (SACZ, Carvalho et al., 2004),
94 which is a main component of the SAMS (Nogués-Paegle et al., 2002; Almeida et al., 2007). The
95 SACZ is an elongated NW-SE band of convective activity that originates in the Amazon Basin,
96 which extends above the northern RdIP drainage basin, and has its southernmost limit in the

97 adjacent SWAO (Carvalho et al., 2004). Thus, the Paraná River discharge is largely determined
98 by the SACZ (Robertson and Mechoso, 2000).

99 The RdIP is an extremely dynamic system which exhibits complex hydrodynamic features
100 associated with the climatic pattern that affect the wind and oceanographic systems, as well as
101 the river discharge (Piola et al., 2008). As mentioned above, a natural intra-annual variability
102 exists with a higher river discharge during the summer season (Depetris and Pasquini, 2007).
103 Besides, a northerly wind pattern during summer leads to a southward and offshore displacement
104 of the low-salinity RdIP freshwater plume (Guerrero et al., 1997; Möller et al., 2008; Piola et al.,
105 2008). In contrast during the winter season, existed a lower RdIP discharge, but exists a
106 predominant southerly wind pattern (associated with a northward displacement of the
107 Westerlies). This situation forces a northward displacement of the RdIP plume and thus,
108 considerably diminishes the salinity on the southern Brazilian continental shelf (Guerrero et al.,
109 1997; Camilloni, 2005; Möller et al., 2008; Piola et al., 2008).

110 The regional climatic system also exhibits an inter-annual and inter-decadal variability,
111 associated with environmental changes (expressed mainly in precipitation patterns) related to the
112 El Niño/La Niña Southern Oscillation (ENSO) and the Pacific Decadal Oscillation (PDO),
113 respectively (Depetris and Kempe, 1990; Depetris et al., 2003; Depetris and Pasquini, 2007;
114 Garreaud et al., 2009; Barreiro, 2010). PDO is associated with ENSO as both seem to produce
115 similar climatic effects, though their mechanisms are not yet fully understood (Garreaud et al.,
116 2009). In this sense, it has been suggested that during both the warm El Niño and the positive
117 PDO phases, there is an increasing trend in precipitations over the RdIP drainage basin
118 associated with an intensification of the SAMS, which leads to a higher RdIP river discharge,
119 while the opposite trend was observed for the negative phases (Ciotti et al., 1995; Depetris and
120 Pasquini, 2007; Garreaud et al., 2009; Barreiro, 2010; García-Rodríguez et al., 2014). However,
121 Piola et al (2005) reported strong NE winds during El Niño conditions which compensate the
122 effect of the positive precipitation anomalies, and thus prevent an anomalous northeastward
123 displacement of the RdIP plume. In addition, there is evidence that the interannual variability in
124 the RdIP drainage basin has a stronger influence on the Uruguay River discharge, whilst the
125 decadal variability is most pronounced in the Paraná River supply (Robertson and Mechoso,
126 2000). Furthermore, Chiessi et al. (2009) found evidence that the Atlantic Multidecadal

127 Oscillation (AMO) influences SAMS intensity on the multidecadal time scales.

128 Regarding the Late Holocene period, a significant number of studies has described the climatic
129 history of South America over the last 1500 cal yr BP (calibrated thousands of years before
130 present), i.e., for the Medieval Climatic Anomaly (MCA, 800-1300 AD) and the Little Ice Age
131 (LIA, 1400-1800 AD), (Cioccale, 1999; Iriondo, 1999; Piovano et al., 2009; del Puerto et al.,
132 2011; Vuille et al., 2012; del Puerto et al., 2013; Salvatecci et al., 2014). These climatic changes
133 have affected the precipitation pattern over South America with regional differences. For eastern
134 Uruguay, this means a warmer and more humid pulse during the MCA, while in the LIA, a drier
135 and colder climate was recorded (del Puerto et al., 2013). Piovano et al. (2009) have inferred
136 similar climatic conditions for the northeastern region of Argentina. In contrast, the opposite
137 pattern was reported for southern Chile and Argentina, where a dry period occurred during the
138 MCA, and a wetter pulse governed the LIA (Haberzettl et al., 2005). Furthermore, Vuille et al.
139 (2012) inferred similar conditions for southeastern Brazil as Haberzettl et al. (2005).

140 Nevertheless, little is known about how the natural climatic variability over South America
141 affects sedimentation, salinity and river discharge on the continental shelf in front of the RdIP,
142 during the Late Holocene period (Burone et al., 2012; Perez et al., in press). The aim of this
143 study therefore, is to determine the variations in the terrigenous sediment input into the ocean
144 over the last 1200 cal yr BP. To determine how the continental influence competed with the
145 marine regime, a 10-m long sediment core was taken from a confined mud depocenter on the
146 inner Uruguayan continental shelf (GeoB 13813-4, Fig. 1). The sedimentary succession of this
147 core was analyzed for major chemical elements (Ca, Ti, Al, Fe, and K) and compared with
148 previously published data of the diatom salinity-indicative groups, i.e. freshwater (F) and marine,
149 marine-brackish (M-B), (Perez et al. in press) in order to assess variations in continental
150 influence.

151 2 Study Area

152 The study area is located on the Uruguayan inner continental shelf hosting the RdIP mud
153 depocenter (50 m water depth, Fig. 1a, b). This silty clay depocenter (Martins and Urien, 2004;
154 Lantzsch et al., 2014) is the result of regional paleogeographic evolution and is associated with
155 deposits of fluvial origin (Urien and Ewing, 1974). The depocenter built up inside the RdIP

156 paleo-valley which was incised by the Paleo-Paraná River during lower sea levels (Masello and
157 Menafra, 1998; Martins et al., 2003; Lantzsch et al., 2014; Hanebuth et al., in press). The RdIP
158 paleo-valley depression offers an effective protection against the generally strong hydrodynamic
159 conditions on the shelf, thus favoring the deposition and preservation of these muds (Fig. 1b).

160 **3 Materials and Methods**

161 A 1028-cm long sediment core (GeoB 13813-4) was taken from the RdIP mud depocenter
162 (34°44'13" S, 53°33'16" W) during research cruise M76/3a with the German research vessel
163 “Meteor” in July 2009 (Krastel et al., 2012; Fig. 1a). During this expedition, sub-bottom
164 profiling with the shipboard PARASOUND system (4 kHz) showed an elongated depression on the
165 seafloor corresponding to the RdIP paleo-valley filled with a complex pattern of acoustic facies
166 (Fig. 1b, Krastel et al., 2012; Lantzsch et al., 2014).

167 **3.1 Age-depth model and sedimentation rates**

168 Material from bivalve shells collected from six sediment samples, distributed evenly over the
169 core and preserved in life position, were used for radiocarbon dating (^{14}C), (Tab.1). The samples
170 were analyzed using AMS- ^{14}C (accelerated mass spectrometry) at the Poznan Radiocarbon
171 Laboratory in Poland. The age depth model was then generated by using the free software Bacon
172 (Blaauw and Christen, 2011, Fig. 2). The raw ^{14}C dates were calibrated using the calibration
173 curve Marine13 (Reimer et al., 2013, cc=2) integrated into this program, and the weighted
174 average ages are expressed in table 1 (Blaauw and Christen, 2011).

175 Bacon software is an approach for developing an age-depth model that uses Bayesian statistics to
176 reconstruct Bayesian accumulation histories for sedimentary deposits. Bacon divides a sediment
177 core into vertical sections (5 cm thick), and estimates the sedimentation rate (years/cm) for each
178 section through millions of Markov Chain Monte Carlo (MCMC) iterations.

179 **3.2 Paleo-environmental proxies**

180 The two methodological approaches combined in this study were chosen according to previous
181 successful applications for inferring continental versus marine influences in the Atlantic Ocean,
182 (Romero et al., 1999; Chiessi et al., 2009; Mahiques et al., 2009; Govin et al., 2012; Burone et

183 al., 2013; Perez et al., in press), as indicated below.

184 3.2.1 Runoff-indicative element ratios

185 The relative concentrations (expressed in counts per second, cps) of the major chemical elements
186 used in this study (Ca, Ti, Fe, K, Al) were obtained by an X-ray fluorescent (XRF) sediment core
187 scanner AVAATECH at MARUM, University of Bremen. XRF core scanning is a fast, non-
188 destructive technique, which allows for the detection of a large number of chemical elements
189 (Löwemark et al., 2011). This technique does not measure absolute element concentrations, but
190 relative intensities. As a consequence, the intensities of the elements are influenced by numerous
191 factors such as water content and sediment density, organic matter content, grain size, biogenic
192 contributions, and carbonate dissolution (Weltje and Tjallingii, 2008). For that reason, it is
193 unwise to use single element intensities, and it is more appropriate to use element ratios to
194 normalize the data (Weltje and Tjallingii, 2008; Francus et al., 2009; Govin et al., 2012). Core
195 GeoB 13813-4 was scanned in 1-cm steps throughout, and the Ti/Ca, Fe/Ca, Fe/K and Ti/Al
196 element ratios were used.

197 Ti, Fe and Al are elements related to aluminosilicates, and associated with clay minerals carried
198 from the continent as weathering products, and through river discharge enters into the ocean
199 (Goldberg and Arrhenius, 1958; Jansen et al., 1992; Yarincik et al., 2000). Therefore these
200 elements vary with the terrigenous portion in offshore sediment (Martins et al., 2007; Burone et
201 al., 2013). Most of the K in marine sediments is also associated with terrigenous materials
202 (Goldberg and Arrhenius, 1958), and occurs mainly in the more arid regions where chemical
203 weathering rates are lower (Govin et al., 2009). In contrast, Ca mainly reflects the marine
204 carbonate content in the sediment, and is thus associated with the local marine productivity
205 (Haug et al., 2001; Salazar et al., 2004; Gonzalez-Mora and Sierro, 2007). Al, Ti and K are little
206 affected by biological and redox variations, whilst Fe is sometimes altered by redox processes
207 (Löwemark et al., 2011; Jansen et al., 1992; Yarincik et al., 2000). Burone et al. (2013) recorded
208 a decreasing seaward gradient in Ti, Fe, Al from a superficial sediment transect from the inner
209 RdIP off to the shelf, while they observed the opposite trend for Ca.

210 Numerous studies used major elements in marine sediments to reconstruct climatic history, but

211 the choice of particular element ratios and the interpretation of such proxies varies from site to
212 site (Govin et al., 2012). Ti/Ca and Fe/Ca ratios were widely used to reconstruct the continental
213 versus the marine influence in the SWAO region (Chiessi et al., 2009; Mahiques et al., 2009;
214 Govin et al., 2012; Bender et al., 2013; Burone et al., 2013). On the other hand, Fe/K and Ti/Al
215 ratio was used in South America to reflect the degree of chemical weathering in areas without
216 significant eolian input (Govin et al., 2012), such as the case of the RdIP (Mahowald et al.,
217 2006). As a consequence of the mentioned above, we used element ratios (Ti/Ca, Fe/Ca, Ti/Al,
218 Fe/K) as regional proxies for the fluvial input signal on the inner Uruguayan continental shelf.

219 3.2.2 Salinity-indicative diatom groups

220 Samples for diatom analyses were first chemically treated (with the aim of cleaning the material
221 from carbonates, organic matter and clay particles) as explain in Perez et al. (in press). Diatom
222 samples were first treated with $\text{Na}_2\text{P}_2\text{O}_7$ to deflocculate the sediment and eliminate clay particles.
223 The samples were then treated with a 35 % HCl to remove inorganic carbonate material. Finally,
224 the samples were boiled in 30 % H_2O_2 for two hours to eliminate organic matter (Metzeltin and
225 García-Rodríguez, 2003). Between each treatment, samples were rinsed at least four times with
226 distilled water. Permanent sediment slides were mounted using the Entellan® mounting medium.
227 A minimum of 400 valves was counted on each slide with a light microscope at 1250 x
228 magnification. The diatoms were then identified and counted at 10 cm depth intervals throughout
229 the sediment core and in 1 cm steps within the uppermost 100 cm. Diatom species were
230 identified and separated into two groups according to their ecological salinity preference, i.e., in
231 groups indicating freshwater (F) and marine/marine-brackish (M-B) conditions, according to
232 Frenguelli (1941, 1945), Müller-Melchers (1945, 1953, 1959), Hasle and Syversten (1996),
233 Witkowski et al. (2000), Metzeltin and García-Rodríguez (2003), Metzeltin et al. (2005), Hassan
234 et al. 2010, Sar et al. (2010) and other standard diatom literature (Perez et al., in press).

235 Romero et al. (1999) determined variations in the continental water discharge by using
236 freshwater diatoms (especially from the genus *Aulacoseira*) along a sediment surface transect
237 from the eastern South Atlantic coast to the open ocean. The same approach was also used in this
238 study to evaluate the freshwater influx on the inner continental shelf.

239 4 Results

240 4.1 Age-depth model and sedimentation rates

241 The core's base was dated to 1200 cal yr BP (750 AD), while a sample at 255 cm was dated to
242 230 cal yr BP (1700 AD, Table 1). The sedimentation rate varied between 0.68 and 1.0 cm yr⁻¹,
243 with a mean sedimentation rate of 0.8 cm yr⁻¹. Minimum values were observed in the top section
244 (i.e., at 200 to 350 cm) and in the bottom section (i.e., at 705 to 967 cm), while the highest values
245 were observed in the middle of the core (at 500 to 705 cm).

246 4.2 Paleo-environmental proxies

247 4.2.1 Runoff-indicative element ratios

248 All the element ratios (Ti/Al, Fe/K, Ti/Ca and Fe/Ca) showed similar profiles (Fig. 3). The
249 lowest values were recorded between 850-1300 AD (coinciding with the MCA), and remained
250 stable during this interval of time. In contrast, high values were recorded from 1300 to 1850 AD
251 (associated with the LIA) and showed a high variability with a number of sharp maxima. In that
252 sense, for the Ti/Al and Fe/K ratios we recorded, a succession of peaks and lows approximately
253 every 100 years (from 1300 to 1500 AD) and every 50 years (1500 AD up to the present), (Fig.
254 3). Moreover during the last century, all element ratios showed a rapid increase toward the
255 highest measured values, most pronounced over the last 50 years (Fig. 3).

256 4.2.2 Salinity-indicative diatom groups

257 Regarding the salinity-indicative diatom groups as shown in Perez et al. (in press), the profile of
258 Group F seems to generally run parallel to those of the four element ratios with lower
259 percentages around 20 % during the MCA times, and higher up to 60 %, rising and more variable
260 values during the LIA period (Fig. 3). An exception is observed for the last 50 yr BP where the
261 percentages declined rapidly towards the former values counted for the MCA time interval. In
262 contrast, the Group M-B ranged from 30 to 80 % generally describing the expected opposite
263 trend compared to the F group (Fig. 3). Over the last 100 yr BP (1900 AD up to the present), an
264 increasing rapid trend coincides with the highest values shown for the element ratios (Fig. 3).

265 **5 Interpretation and Discussion**

266 **5.1 Age-depth model and sedimentation rates**

267 The RdIP mud depocenter shows an exceptionally high sedimentation rate (0.8 cm yr⁻¹ on
268 average) compared with other records from the southern Brazilian continental shelf (Mahiques et
269 al., 2009; Chiessi et al., 2014). This high sedimentation rate is probably a consequence of the
270 enormous amount of sediment transported by the Paraná and Uruguay Rivers into the RdIP
271 watershed and further onto the Uruguayan shelf (Lantzsch et al., 2014). In addition, an
272 amplification of the sedimentation rate could be a consequence of the fact that the RdIP paleo-
273 valley depression offers protection against strong hydrodynamic conditions on the shelf, favoring
274 the deposition of sediments (Lantzsch et al., 2014; Hanebuth et al., in press). **The beginning of**
275 **sedimentation** is possibly associated with the establishment of humidity conditions in the Late
276 Holocene which have resulted in an increasing RdIP River discharge, as well as a significant
277 sedimentation of terrigenous material over the RdIP paleo-valley (Urien et al., 1980; Iriondo,
278 1999; Mahiques et al., 2009; Lantzsch et al., 2014).

279 **5.2 Paleo-environmental proxy records**

280 The proxy data used in this study are correlated positively with each other (**excluding the last**
281 **century**), and reveal the direct influence of the RdIP as a source of terrigenous sediments within
282 the inner Uruguayan continental shelf.

283 The element ratios Ti/Ca and Fe/ Ca indicates, as do other geochemical and biological proxies
284 (Perez et al., in press), a mixed fluvio-marine signal on the inner Uruguayan continental shelf,
285 spanning over the last 1200 years. **Ti and Fe are supplied from the RdIP watershed (Depetris et**
286 **al., 2003), whilst Ca is an element associated with calcareous organisms such as small mollusks,**
287 **forams and coccolithophorides in the ocean sediment, and therefore is related to the marine-**
288 **biogenic productivity of the continental shelf (Depetris and Pasquini, 2007; Govin et al., 2012;**
289 **Razik et al., 2013). Thus the variability of these element ratios indicates different degrees of**
290 **continental influence in the study area during the Late Holocene.**

291 The results of the proxies integral analysis have been linked to general climatic changes that

292 have occurred on a regional to global scale (Fig.3), and allow us to infer three major time
293 intervals, i.e., the MCA, the LIA and the current warm period (Mann et al. 2009), all of which
294 were characterized by changing continental versus marine influences in the study area.

295 The oldest recorded period, from 800 to 1300 AD, is closely associated with the MCA (reported
296 as a positive temperature anomaly in the northern hemisphere, Bradley et al., 2008; Mann et al.,
297 2009). During this period, a strong and steady influence of marine conditions governed the inner
298 Uruguayan continental shelf (inferred by low values of Ti/Ca and Fe/Ca, and a dominance of the
299 M-B diatom salinity group), probably as a result of a weakened RdIP water and terrigenous
300 sediment discharge. This situation led to a major **and more constant** sedimentation of marine
301 particulate carbon during the MCA (Perez et al., in press). In addition, the low Fe/K values
302 registered during the MCA would suggest conditions of reduced RdIP river discharge and dry
303 conditions over the drainage basin (Vuille et al., 2012). **Climatically drier conditions would
304 decrease chemical weathering in the Fe-rich RdIP drainage basin, thus decreasing the Fe content
305 in the offshore depocenters in relation to K which is associated with drier conditions (Depetris et
306 al., 2003; Depetris and Pasquini et al., 2007).**

307 Our findings, combined with those reported in other studies, suggest that a northward
308 displacement of the ITCZ and a weakened SAMS could have taken place during the MCA (Bird
309 et al., 2011a; Bird et al., 2011b; Vuille et al., 2012; Apaéstegui et al., 2014; Salvatecci et al.,
310 2014). **Though the continental SAMS has spatial-temporal characteristics that differ from the
311 maritime ITCZ, the latitudinal position of the ITCZ is closely related to changes in the SAMS
312 intensity, and both climatic elements also respond to temperature anomalies in the northern
313 hemisphere (Stríkis et al., 2011; Vuille et al., 2012).** In this sense, positive/negative northern
314 hemisphere temperature anomalies are linked to the north/south directional migration of the
315 ITCZ **and diminishing/increasing SAMS activity** (Broccoli et al., 2006; Bird et al., 2011b; **Stríkis
316 et al., 2011; Vuille et al., 2012).** **Thus, the positive temperature anomalies in the northern
317 hemisphere during the MCA (Mann et al., 2009; probably associated with a positive phase of the
318 AMO), would have led to reduced SAMS and SACZ intensity, in addition to a northward
319 displacement of the ITCZ (Chiessi et al., 2009; Stríkis et al., 2011; Vuille et al., 2012). Such
320 atmospheric conditions during the MCA would have led to a significant decrease in rainfall over
321 the RdIP watershed (mainly in the catchment area of its main tributary, the Paraná River;**

322 Robertson and Mechoso, 2000). As a consequence of this, we inferred a reduction in both
323 freshwater and sediment input, in conjunction with an increase in salinity (Perez et al., in press)
324 on the Uruguayan continental shelf. The decrease in SACZ activity during the MCA could also
325 help to explain the more humid conditions inferred for Uruguay during this episode (del Puerto
326 et al., 2013). This is associated with an increase in precipitation over the Uruguay River drainage
327 basins due to a reduced SACZ intensity as discuss below (Robertson and Mechoso, 2000).

328 The following period, from 1300 to 1850 AD, coincided with the LIA as reported for the
329 northern hemisphere (Bradley et al., 2003; Mann et al., 2009). This period is characterized by
330 higher values of Ti/Al, Fe/K, Ti/Ca and Fe/Ca than those recorded during the preceding period.
331 Therefore, we recorded a higher content of terrigenous material rich in Ti and Fe from the RdIP
332 watershed (Depetris et al., 2003; Depetris and Pasquini, 2007) which is associated with a higher
333 river discharge during the LIA (Fig. 4). Furthermore, a dominance of F diatoms (Fig. 3) was
334 detected. The F diatom group was mainly dominated by *Aulacoseira* spp., especially *A.*
335 *granulata* (Perez et al., in press), which is the most common diatom genus from the Paraná River
336 and the inner RdIP (Gomez and Bauer, 2002; Licursi et al., 2006; Devercelli et al., 2014).
337 Moreover, Massaferro et al. (2014) observed that the F diatom group recorded in the uppermost
338 55 cm of the sediment core GeoB 13813-4 was associated with the positive anomalies of the
339 Paraná River discharges. Thus, all the proxies indicate wetter conditions over the RdIP drainage
340 basin, and consequently, a major freshwater supply from the RdIP to the inner Uruguayan shelf
341 during the LIA. Accordingly, we observed the highest rates of terrigenous deposition during this
342 episode.

343 The LIA, characterized by cold conditions over the northern hemisphere, was then related to a
344 southward displacement of the ITCZ and a strengthening of SAMS and SACZ (Bird et al.,
345 2011b; Vuille et al., 2012). This leads to both a reduction in rainfall rates over northern South
346 America, Central America and Mexico (Haug et al., 2001; Vazques-Castro et al., 2008), and
347 elevated rainfall rates in the Andes (Sifeddine et al., 2008; Bird et al., 2011a; Bird et al., 2011b;
348 Vuille et al., 2012; Apaéstegui et al., 2014; Salvatecci et al., 2014), and over SESA (Meyer and
349 Wagner, 2009; Vuille et al., 2012). The intensification and northward displacement of the
350 Southern Westerlies during the LIA was also registered (Moy et al., 2009; Koffman et al., 2014).
351 This, in conjunction with a higher river discharge, would have also caused an anomalous

352 northward shift of the RdIP river plume. Such atmospheric conditions during the LIA would
353 have led to a significant increase in rainfall over the RdIP watershed. Therefore, the outcome was
354 a higher influence of the RdIP river plume within the inner Uruguayan continental shelf as
355 recorded in this study.

356 The succession of peaks and lows in the element ratios from 1300 AD to present (every 50 to
357 100 years), probably suggest an influence of the AMO on RdIP river discharge related to changes
358 in SAMS and SACZ intensity (Chiessi et al., 2009; Strikis et al., 2011). The AMO significantly
359 affects the SAMS on multi-decadal time scales, leading to a reduced SAMS intensity when the
360 AMO is in its positive phase, and the ITCZ retreats northward, leading to a decrease in RdIP
361 river discharge (Chiessi et al., 2009; Strikis et al., 2011; Bird et al., 2011b). Chiessi et al. (2009)
362 proposed that sea surface temperature and atmospheric circulation anomalies triggered by the
363 AMO would control the variability in SAMS and SACZ intensity.

364 An increase in SACZ intensity during the LIA and its decrease during the MCA, inferred through
365 this study, could explain the contrasting spatial/temporal climatic conditions recorded in the two
366 regions in the RdIP drainage basin (Vuille et al., 2012; del Puerto et al., 2013). SACZ intensity is
367 associated with an enhanced river runoff in the northern region of the RdIP catchment area
368 (Paraná River) and a diminished runoff in the southern area (Uruguay River; Robertson and
369 Mechoso, 2000). This north/south river runoff contrast, in response to an intensified/weakened
370 SACZ, would tend to transport less/more moisture over the Uruguay River basin, thus leading to
371 an increase/decrease in precipitation during MCA/LIA over Uruguay (del Puerto et al., 2013).

372 Finally, the latest period started around 1850 AD, and is characterized by a sharp global increase
373 in temperature due to significant human impact (Crutzen, 2006; Halpern et al., 2008; Hoegh-
374 Guldberg and Bruno, 2010; Mauelshagen, 2014). Our sediment record for the last century bears
375 witness to a high river discharge as the highest element ratios were recorded, whilst the diatom
376 record shows a dominance of the M-B species, typical of marine-estuarine conditions. We make
377 the assumption that such a unique incongruence, compared with a optimal positive correlation
378 for the preceding time intervals, is not only a consequence of the regional anthropogenic impact
379 (Depetris and Pasquini, 2007; Bonachea et al., 2010, García-Rodríguez et al., 2010), as already
380 reported by Perez et al., (in press), but also that of natural changes associated with an increasing

381 Paraná river runoff after 1970 (Marrero et al., submitted).

382 **6 Conclusions**

383 The observed changes in the presented proxy records indicate variations in both the continental
384 runoff and the marine influence, related to regional climatic variability. Therefore, we put
385 forward the suggestion that global atmospheric changes (latitudinal shifts of the ITCZ, related to
386 changes in **SAMS and SACZ intensity**) have made an impact on the hydrodynamics and
387 consequently, on the local sedimentation regime, on the inner Uruguayan continental shelf over
388 the past 1200 cal yr BP (750-2000 AD).

389 During the MCA (800-1300 AD) a northward shift of the ITCZ **and a reduction in SAMS and**
390 **SACZ activities** would have caused a decrease in the rainfall rate over the RdIP drainage basin,
391 resulting in more estuarine-marine conditions predominating over a freshwater plume signal.
392 During the LIA (1400-1800 AD) in contrast, a southward shift of the ITCZ **and a strengthening**
393 **in SAMS and SACZ activities** would have led to an increased precipitation over the RdIP
394 drainage basin, reflected by stronger terrigenous influences in terms of freshwater supply on the
395 inner Uruguayan shelf. **Furthermore, a possible multi-decadal oscillation probably associated**
396 **with AMO since 1300 AD, reflects the variability in both the SASM and SACZ systems.**

397 **7 Acknowledgements**

398 We would like to express special thanks to Ines Sunesen, Eugenia Sar, M. Michel Mahiques and
399 Carina Lange for their fruitful discussions. We would also like to thank Vivienne Pettman for her
400 very valuable suggestions for improving the English **and also the reviewers for their critical**
401 **comments and suggestions which undoubtedly improved the manuscript content.** We
402 acknowledge PEDECIBA (Programa para el Desarrollo de las Ciencias Básicas) Geociencias,
403 ANII (Agencia Nacional de Investigación e Innovación), DAAD (German Academic Exchange
404 Service), and RLB (Red Latinoamericana de Botanica) for their financial support. **The authors**
405 **would also like to thank to PAGES for their partially financial support of this publication.** This
406 article is an outcome of the MARUM SD2 projectas part of the DFG 543 Research
407 Center/Excellence Cluster “The Ocean in the Earth System” at the University of Bremen.

408 **8 References**

409 Acha, E., Mianzan, H., Iribarne, O., Gagliardini, D., Lasta, C., and Daleo, P.: The role of
410 the Río de la Plata bottom salinity front in accumulating debris, *Mar. Poll. Bull.*, 46, 197-202,
411 2003.

412 Almeida, R. A. F., Nobre, P., Haarsma, R. J., and Campos, E. J. D.: Negative ocean-
413 atmosphere feedback in the South Atlantic Convergence Zone, *Geophys. Res. Lett.*, 34, L18809,
414 doi:10.1029/2007GL030401, 2007.

415 Apaéstegui, J., Cruz, F. W., Sifeddine, A., Vuille, M., Espinoza, J. C., Guyot, J. L.,
416 Khodri, M., Strikis, N., Santos, R. V., Cheng, H., Edwards, L., Carvalho, E., and Santini, W.:
417 Hydroclimate variability of the northwestern Amazon Basin near the Andean foothills of Peru
418 related to the South American Monsoon System during the last 1600 years, *Clim. Past.*, 10,
419 1967–1981, 2014.

420 Barreiro, M.: Influence of ENSO and the South Atlantic Ocean on climate predictability
421 over Southeastern South America, *Clim. Dyn.*, 35, 1493-1508, doi:10.1007/S00382-009-0666-9,
422 2010.

423 Bender, V. B., Hanebuth, T. J. J., and Chiessi, C. M.: Holocene shifts of the subtropical
424 shelf front off Southeastern South America controlled by high and low latitude atmospheric
425 forcings, *Paleoceanography*, 28, 1-10, doi: 10.1002/palo.20044, 2013.

426 Bird, B. W., Abbott, M. B., Rodbell, D. T., and Vuille, M.: Holocene tropical South
427 American hydroclimate revealed from a decadal resolved lake sediment $\delta^{18}\text{O}$ record, *Earth
428 Planet. Sc. Lett.*, 310, 192–202, 2011a.

429 Bird, B. W., Abbott, M. B., Vuille, M., Rodbell, D. T., Stansella, N. D., and
430 Rosenmeiera, M. F.: 2,300-year-long annually resolved record of the South American summer
431 monsoon from the Peruvian Andes, *PNAS*, 108, 8583–8588, 2011b.

432 Bisbal, G. A.: The southeast South American shelf large marine ecosystem: Evolution
433 and components, *Mar. Policy*, 19, 1, 21-38, 1995.

434 Blaauw, M., and Christen, J. A.: Flexible paleoclimate age-depth models using an
435 autoregressive gamma process, *Bay. Anal.*, 6, 457-474, 2011.

436 Bonachea, J., Bruschi, V. M., Hurtado, M. A., Forte, L. M., da Silva, R., Etcheverry, M.,
437 Cavallotto, J. L., Dantas, M. F., Pejon, O. J., Zuquette, L. Z., Bezerra, M. A. O., Remondo, J.,
438 Rivas, V., Gómez-Arozamena, J., Fernández, G., and Cendrero, A.: Natural and human forcing
439 in recent geomorphic change; case studies in the Rio de la Plata basin, *Sci. Total Environ.*, 408,
440 2674-2695, doi:10.1016/J.SCITOTENV.2010.03.00, 2010.

441 Bradley, R. S., Hughes, M. K., and Diaz, H. F.: Climate in Medieval Time, *Science*, 302,
442 404-405, 2008.

443 Broccoli, A. J., Dahl, K. A, and Stouffer, R. J.: Response of the ITCZ to Northern
444 Hemisphere cooling, *Geophys. Res. Lett.*, 33, L01702, doi:10.1029/2005GL024546, 2006.

445 Burone, L., Centurión, V., Cibils, L., Franco-Fraguas, P., García-Rodríguez, F., García,
446 G., and Pérez, L.: Sedimentología y Paleooceanografía, in: Programa oceanográfico de
447 caracterización del margen continental uruguayo-ZEE, edited by: Burone, L., Montevideo,
448 Uruguay, 240-295, 2012.

449 Burone, L., Ortega, L., Franco-Fraguas, P., Mahiques, M., García-Rodríguez, F.,
450 Venturini, N., Marin, Y., Brugnoli, E., Nagai, R., Muniz, P., Bicego, M., Figueira, R., and
451 Salaroli, A.: A multiproxy study between the Río de la Plata and the adjacent South-western
452 Atlantic inner shelf to asses the sediment footprint of river vs. marine influence, *Cont. shelf Res.*,
453 55, 141-154, 2013.

454 Camilloni, I.: Variabilidad y tendencias hidrológicas en la cuenca del Plata, in: El cambio
455 climático en el Río de la Plata, edited by: Barros, V., Menendez, A. and Nagy, G., CIMA,
456 Buenos Aires, 20-31, 2005.

457 Carvalho, L. M. V., Jones, C., and Liebmann, B.: The South Atlantic Convergence Zone:
458 Intensity, Form, Persistence, and Relationships with Intraseasonal to Interannual Activity and
459 Extreme Rainfall, *J. Climate*, 17, 88–108, 2004.

460 Chiessi, C. M., Mulitza, S., Patzold, J., Wefer, G., and Marengo, J. A.: Possible impact of
461 the Atlantic Multidecadal Oscillation on the South American summer monsoon. *Geophys. Res.*
462 *Lett.*, 36, L21707, doi:10.1029/2009GL039914, 2009.

463 Chiessi, C. M., Mulitza, S. G., Jeroen, S. J. B., Campos, M. C., and Gurgel, M. H. C.:
464 Variability of the Brazil Current during the late Holocene, *Palaeogeogr. Palaeocl.*, 415, 28–36,

465 doi: 10.1016/j.palaeo.2013.12.005, 2014.

466 Cioccale, M.: Climatic conditions in the central region of Argentina in the last 1000
467 years, *Quat. Int.*, 62, 35-47, 1999.

468 Ciotti, A. M., Odebrecht, C., Fillmann, G., and Moller, O. O.: Freshwater outflow and
469 Subtropical Convergence influence on phytoplankton biomass on the southern Brazilian
470 continental shelf, *Cont. Shel. Res.*, 15, 14, 1737-1756, 1995.

471 Crutzen, P. J.: The “Anthropocene”, in: *Earth System Science in the Anthropocene*,
472 edited by: Ehlers, E. and Krafft, T., Springer Berlin Heidelberg, 13-18, doi 10.1007/3-540-
473 26590-2, 2006.

474 del Puerto, L., García-Rodríguez, F., Bracco, R., Castiñeira, C., Blasi, A., Inda, H.,
475 Mazzeo, N. and Rodríguez, A.: Evolución climática holocénica para el sudeste de Uruguay,
476 Analisis multi-proxy en testigos de lagunas costeras, in: *El Holoceno en la zona costera de*
477 *Uruguay*, edited by: García-Rodríguez, F., Universidad de la Republica (UdelaR), 117-154,
478 2011.

479 del Puerto, L., Bracco, R., Inda, H., Gutierrez, O., Panario, D., and García-Rodríguez, F.:
480 Assessing links between late Holocene climate change and paleolimnological development of
481 Peña Lagoon using opal phytoliths, physical, and geochemical proxies, *Quat. Int.*, 287, 89-100,
482 doi:10.1016/j.quaint.2011.11.026, 2013.

483 Depetris, P.J. and Kempe, S.: The impact of the El Niño 1982 event on the Paraná River,
484 its discharge and carbon transport. *Palaeogeogr. Palaeoclimatol.*, 89, 239-244, 1990.

485 Depetris, P. J. and Pasquini, A. I.: Discharge trends and flow dynamics of southern
486 southamerican rivers draining the southern Atlantic seabord: an overview, *J. Hidrol.*, 333, 385-
487 399, doi: 10.1016/j.hydrol.2006.09005, 2007.

488 Depetris, P. J., Probst, J-L., Pasquini, A. I. and Gaiero, D. M.: The geochemical
489 characteristics of the Paraná River suspended sediment load: an initial assessment, *Hydrol.*
490 *Process*, 17, 1267–1277, doi: 10.1002/hyp.1283, 2003.

491 Devercelli, M., Zalocar de Domitrovic, Y., Forastier, M. E. and Meichtry de Zaburlín N.:
492 Phytoplankton of the Paraná River Basin, *Advanc. Limnol.*, 65, 39–65, doi: 10.1127/1612-

493 166X/2014/0065-0033, 2014.

494 Francus, P., Lamb, H., Nakawaga, T., Marshall, M., and Brown, E.: The potential of high
495 resolution X-ray fluorescence core scanning: Applications in paleolimnology, *PAGES news* 17, 9,
496 93-95, 2009.

497 Frenguelli, J.: Diatomeas del Río de la Plata, *Revista Museo Nacional La Plata*, III, 213-
498 334, 1941.

499 Frenguelli, J.: Diatomeas del Platense, *Revista Museo Nacional La Plata*, III, 77-221,
500 1945.

501 FREPLATA: Análisis Diagnóstico Transfronterizo del Río de la Plata y su Frente
502 Marítimo. Documento Técnico. Proyecto “Protección Ambiental del Río de la Plata y su Frente
503 Marítimo: Prevención y Control de la Contaminación y Restauración de Hábitats”. Proyecto
504 PNUD/GEF/RLA/99/G31, 106, 2004.

505 Garcia, S. and Kayano, M.: Some evidence on the relationship between the South
506 American monsoon and the Atlantic ITCZ, *Theor. Appl. Climatol.*, 99, 29–38, 2010.

507 García-Rodríguez, F., Hutton, M., Brugnoli, E., Venturini, N., del Puerto, L., Inda, H.,
508 Bracco, R., Burone, L., and Muniz, P.: Assessing the effect of natural variability and human
509 impacts on the environmental quality of a coastal metropolitan area (Montevideo Bay, Uruguay),
510 *PANAMJAS*, 5, 1, 90–99, 2010.

511 García-Rodríguez, F., Brugnoli, E., Muniz, P., Venturini, N., Burone, L., Hutton, M.,
512 Rodríguez, M., Pita, A., Kandravicius, N., Perez, L., and Verocai, J.: Warm-phase ENSO
513 events modulate the continental freshwater input and the trophic state of sediments in a large
514 South American estuary. *Mar. Freshwater Res.*, 65, 1-11, 2014.

515 Garreaud, R. D., Vuille, M., Compagnucci, R., and Marengo, J.: Present-day South
516 American climate, *Palaeogeogr. Palaeoclimatol.*, 281, 3-4, 180-195, 2009.

517 Giberto, D. A., Bremec, C. S., Acha, E. M., and Mianzan, H.: Large-scale spatial patterns
518 of benthic assemblages in the SW Atlantic: the Río de la Plata, *Estuar. Coast. Shelf S.*, 61, 1-13,
519 2004.

520 **Goldberg, E. D., and Arrhenius, G.O.S.: Geochemistry of pacific pelagic sediments,**

521 **Geochim. Cosmochim. Ac., 13, 153-212, 1958.**

522 Gómez, N. and Bauer, D. E.: Diversidad fitoplanctónica en la franja costera Sur del Río
523 de la Plata, *Biol. Acuát.*, 19, 7-26, 2000.

524 González-Mora, B. and Sierro, F. J.: Caracterización geoquímica de las capas ricas en
525 materia orgánica registradas durante el estadio isotópico marino 7 en el Mar de Alborán
526 (Mediterráneo occidental), *GEOGACETA*, 43, 111-114, 2007.

527 Govin, A., Holzwarth, U., Heslop, D., Ford Keeling, L., Zabel, M., Mulitza, S., Collins, J.
528 A., and Chiessi, C. M.: Distribution of major elements in Atlantic surface sediments (36°N–
529 49°S): Imprint of terrigenous input and continental weathering, *Geochem. Geophys. Geosys*, 13,
530 1, 1525-2027, 2012.

531 Guerrero, R., Acha, E., Framiñan, M., and Lasta, C.: Physical oceanography of the Rio de
532 la Plata Estuary, Argentina, *Cont. Shelf. Res.*, 17, 7, 727-742, 1997.

533 Haberzettl, T., Fey, M., Lucke, A., Maidana, N., Mayr, C., Ohlendorf, C., Schabitz, F.,
534 Schleser, G. H., Wille, M. and Zolitschka, B.: Climatically induced lake level changes during the
535 last two millennia as reflected in sediments of Laguna Potrok Aike, southern Patagonia (Santa
536 Cruz, Argentina), *J. Paleolimnol.*, 33, 283–302, 2005.

537 Halpern, B. S., Walbridge, S., Selkoe, K. A., Kappel, C. V., Micheli, F., D'Agrosa, C.,
538 Bruno, J. F., Casey, K. S., Ebert, C., Fox, H. E., Fujita, R., Heinemann, D., Lenihan, H., Madin,
539 E. M., Perry, M. T., Selig, E., Spalding, M., Steneck, R. and Watson, R.: A Global Map of
540 Human Impact on Marine Ecosystems, *Science*, 319, 948-951, 2008.

541 Hanebuth, T. J. J., Lantzsch, H., García-Rodríguez, F. and Perez, L.: Currents controlling
542 sedimentation: paleo-hydrodynamic variability inferred from the continental-shelf system off SE
543 South America (Uruguay), in: *Ciencias Marino Costeras en el Umbral del Siglo XXI: Desafíos*
544 *en Latinoamérica y el Caribe (XV COLACMAR)*, edited by: Muniz, P., Conde, D., Venturini, N.
545 and Brugnoli, E., in press.

546 Hasle, G. R. and Syvertsen, E. E.: Marine diatoms, in: *Identifying marine phytoplankton*,
547 edited by: Tomas, C. R., Academic Press, San Diego, California, 5-385, 1996.

548 Hassan, G.: Paleocological significance of diatoms in argentinean estuaries, Consejo

549 Nacional de Investigaciones Científicas y Técnicas (CONICET), Argentina, 2010.

550 Haug, G. H., Hughen, K. A., Sigman, D. M., Peterson, L. C. and Rohl, U.: Southward
551 Migration of the Intertropical Convergence Zone Through the Holocene, *Science*, 293, 1304-
552 1307, doi: 10.1126/science.1059725, 2001.

553 Hoegh-Guldberg, O., and Bruno, J. F.: The Impact of Climate Change on the World's
554 Marine Ecosystems, *Science*, 328, 1523-1528, doi: 10.1126/science.1189930, 2010.

555 Iriondo, M.: Climatic changes in the South American plains: Records of a continent-scale
556 oscillation, *Quatern. Int.*, 57-58, 93-112, 1999.

557 Jansen, J. H. F., Van der Gaast, S. J., Koster, B., and Vaars A. J.: CORTEX, a shipboard
558 XRF-scanner for element analyses in split sediment cores, *Mar. Geol.*, 151, 1–4, 143–153,
559 doi:10.1016/S0025 3227(98)00074-7, 1998.

560 Koffman, B. G., Kreutz, K. J., Breton, D. J., Kanel, E. J., Winski, D. A., Birkel, S. D.,
561 Kurbatov, A. V., and Handley, M. J.: Centennial-scale variability of the Southern Hemisphere
562 westerly wind belt in the eastern Pacific over the past two millennia, *Clim. Past*, 10, 1125–1144,
563 doi:10.5194/cp-10-1125-2014, 2014.

564 Krastel, S., Wefer, G., Hanebuth, T. J. J., Antobreh, A. A., Freudenthal, T., Preu, B.,
565 Schwenk, T., Strasser, M., Violante, R., and Winkelmann, D.: Sediment dynamics and
566 geohazards off Uruguay and the de la Plata River region (northern Argentina and Uruguay),
567 *Geo-Mar. Let.*, 31, 4, 271-283, doi: 10.1007/s00367-011-0232-4, 2011.

568 Krastel, S., Wefer, G. and cruise participants: Sediment transport off Uruguay and
569 Argentina: From the shelf to the deep sea. 19.05.2009 – 06.07.2009, Montevideo (Uruguay) –
570 Montevideo (Uruguay), Report and preliminary results of RV METEOR Cruise M78/3, *Berichte*,
571 *Fachbereich Geowissenschaften, Universität Bremen*, 285, 2012.

572 Lantsch, H., Hanebuth, T. J. J., Chiessi, C. M., Schwenk, T., and Violante, R.: A high-
573 supply sedimentary system controlled by strong hydrodynamic conditions (the continental
574 margin off the Plata Estuary during the late Quaternary, *Quat. Res.*, 81, 2, 339-354, 2014.

575 Licursi, M., Sierra, M. V., and Gómez, N.: Diatom assemblages from a turbid coastal
576 plain estuary: Río de la Plata (South America), *J. Marine Syst.*, 62, 33-45, 2006.

577 Löwemark, C., Chen, H., Yang, T-N., Kylander, M., Yu, E-F., Hsu, Y-W., Lee, T-Q.,
578 Song, S-R., and Jarvis, S.: Normalizing XRF scanner data: A cautionary note on the
579 interpretation of high-resolution records from organic-rich lakes, *J. Asia Earth Sci.*, 40, 1250-
580 1256, 2011.

581 Mahiques, M. M., Wainer, I. K. C., Burone, L., Nagai, R., Sousa, S. H. M., Lopes
582 Figueira, R. C., da Silveira, I. C. A., Bicego, M. C., Alves, D. P. V., and Hammer, O.: A high-
583 resolution Holocene record on the Southern Brazilian shelf: Paleoenvironmental implications,
584 *Quatern. Int.*, 206, 52-61, 2009.

585 Mahowald, N. M., Muhs, D. R., Levis, S., Rasch, P. J., Yoshioka, M., Zender, C. S., and
586 Luo, C.: Change in atmospheric mineral aerosols in response to climate: Last glacial period,
587 preindustrial, modern, and doubled carbon dioxide climates, *J. Geophys. Res.*, 111, D10202,
588 doi:10.1029/2005JD006653, 2006.

589 Mann, M. E., Zhang, Z., Rutherford, S., Bradley, R. S., Hughes, M., Shindell, D.,
590 Ammann, D., Faluvegi, G., and Ni, F.: Global Signatures and Dynamical Origins of the Little Ice
591 Age and Medieval Climate Anomaly, *Science*, 326, 1256-1259, 2009.

592 Marrero, A., Tudurí, A., Perez, L., Cuña, C., Muniz, P., Lopes Figueira, C. R., Mahiques,
593 M. M., Pittauerová, D., Hanebuth, T. J. J., and García- Rodríguez, F.: Cambios históricos en el
594 aporte terrígeno de la cuenca del Río de la Plata sobre la plataforma interna uruguaya, LAJSBA,
595 submitted, 2015.

596 Martins, V., Dubert, J., Jouanneau, J.-M., Weber, O., Ferreira da Silva, E., Patinha, C.,
597 Alverinho Dias, J.M., and Rocha, F.: A multiproxy approach of the Holocene evolution of shelf-
598 slope circulation on the NW Iberian continental shelf, *Mar. Geol.*, 239, 1–18, 2007.

599 Martins, L. R., Martins, I. R., and Urien, C. M.: Aspectos sedimentares da plataforma
600 continental na área de influencia de Rio de La Plata, *Gravel*, 1, 68-80, 2003.

601 Martins, L. R. and Urien, C. R.: Areias da plataforma e a erosao costeira, *Gravel*, 2, 4-24,
602 2004.

603 Masello, A. and Menafra, R.: Macrobenthic communities of the Uruguayan coastal zona
604 and adjacent areas, in: *Río de la Plata una revisión ambiental*, edited by: Wells, P. G. and
605 Daborn, G. R., University of Dalhousie, 140-186, 1998.

606 Massaferrero, J., Perez, L., de Porras, M. E., Pérez Becoña, L., Tonello, M., and Juggins,
607 S.: Paleocological data analysis with R, course for Latin American researchers, Pages
608 Magazine, Workshop reports, 22 , 2, 105, 2014.

609 Mauelshagen, F.: Redefining historical climatology in the Anthropocene. The
610 Anthropocene Review, 1, 2, 171-204, doi: 10.1177/2053019614536145, 2014.

611 Metzeltin, D. and García-Rodríguez, F. (Eds): Las Diatomeas Uruguayas, Facultad de
612 Ciencias, Montevideo, Uruguay, 654, 2003.

613 Metzeltin, D., Lange-Bertalot, H. and García-Rodríguez, F. Diatoms of Uruguay -
614 Taxonomy, Biogeography, Diversity, in: Iconographia Diatomologica (15), edited by: Lange-
615 Bertalot, H. and Gantner Verlag, A. R. G., Koenigstein, Germany, 736, 2005.

616 Meyer, I. and Wagner, I.: The Little Ice Age in Southern South America: Proxy and
617 model based evidence, in: Past climate variability in South America and surrounding regions,
618 from the last glacial maximum to the Holocene, edited by: Vimeux, F., Sylvestre, F. and Khodri,
619 M., Springer, 395-412, 2009.

620 Möller, Jr. O. O., Piola, A. R., Freitas, A. C., and Campos, E.: The effects of river
621 discharge and seasonal winds on the shelf off southeastern South America, Cont. Shelf Res., 28,
622 13, 1603-1624, 2008.

623 Moy, C. M., Moreno, P. I., Dunbar, R. B., Kaplan, M. R., Francois, J-P., Villalba, R., and
624 Haberzettl, T.: Climate change in Southern South America during the last two millennia, in: Past
625 climate variability in South America and surrounding regions, edited by: Vimeux, F., Sylvestre,
626 F. and Khodri, M., Developments in Paleoenvironmental Research (14), Springer, 353-393,
627 2009.

628 Müller-Melchers, P.: Diatomeas procedentes de algunas muestras de turba del Uruguay.
629 Comunicaciones Botánicas del Museo de Historia Natural de Montevideo, 1, 17, 1-25, 1945.

630 Müller-Melchers, P.: Sobre algunas diatomeas planctónicas de Atlántida (Uruguay),
631 Physis, 20, 59, 459-466, 1953.

632 Müller-Melchers, P.: Plankton diatoms of the Southern Atlantic of Argentina and
633 Uruguay coast. Comunicaciones Botánicas del Museo de Historia Natural de Montevideo 3, 38,

634 1-53, 1959.

635 Nagai, R. H., Ferreira, P. A. L., Mulkherjee, S., Martins, V. M., Figueira, R. C. L., Sousa,
636 S. H. M. and Mahiques, M. M.: Hidrodinamic controls on the distribution of surface sediments
637 from the southeast South American continental shelf between 23 S and 38 S, *Cont. Shelf. Res.*,
638 89, 51-60, doi.org/10.1016/j.csr.2013.09.016, 2014.

639 Nogués-Paegle, J., Mechoso, C. R., Fu, R., Berbery, E. H., Chao, W. C., Chen, T.-C.,
640 Cook, K., Diaz, A. F., Enfield, D., Ferreira, R., Grimm, A. M., Kousky, V., Liebmann, B.,
641 Marengo, J., Mo, K., Neelin, J. D., Paegle, J., Robertson, A. W., Seth, A., Vera, C. S., and Zhou,
642 J.: Progress in Pan American CLIVAR research: Understanding the South American monsoon.
643 *Meteorologica*, 27, 3-32, 2002.

644 Perez, L., García-Rodríguez, F., and Hanebuth, T.: Paleosalinity changes in the Río de la
645 Plata estuary and on the adjacent Uruguayan continental shelf over the past 1200 cal ka BP: an
646 approach using diatoms as proxy, in: Applications of paleoenvironmental techniques in estuarine
647 studies, *Developments in Paleoenvironmental Research (DPER)*, edited by: Weckström, K.,
648 Saunders, P. and Skilbeck, G., Springer, in press.

649 Piola, A. R., Campos, E. J. D., Möller Jr., O. O., Charo, M., and Martinez C. M.:
650 Subtropical shelf front off eastern South America, *J. Geophys. Res.*, 105, 6566–6578, 2000.

651 Piola, A. R., Moller, O. O., Guerrero, R. A. and Campos, E. J. D.: Variability of the
652 subtropical shelf front off eastern South America: Winter 2003 and summer 2004, *Cont. Shelf*
653 *Res.*, 28, 1639-1648, doi: 10.1016/j.csr.2008.03.013, 2008.

654 Piovano, E. L., Ariztegui, D., Cordoba, F., Cioccale, J. and Sylvestre, F.: Hydrological
655 variability in South America below the tropic of Capricorn (Pampas and Patagonia, Argentina)
656 during the Last 13.0 Ka, in: Past climate variability in South America and surrounding regions,
657 from the last glacial maximum to the Holocene, edited by: Vimeux, F., Sylvestre, F. and Khodri,
658 M., Springer, 323-352, 2009.

659 Razik, S., Chiessi, C. M, Romero, O. E. and von Dobeneck, T.: Interaction of the South
660 American Monsoon System and the Southern Westerly Wind Belt during the last 14 kyr
661 *Palaeogeogr. Palaeocl.*, 374, 28–40, 2013.

662 Reimer, P.J., Bard, E., Bayliss, A., Beck, J.W., Blackwell, P.G., Bronk Ramsey, C.,

663 Buck, C.E., Edwards, R.L., Friedrich, M., Grootes, P.M., Guilderson, T.P., Haflidason, H.,
664 Hajdas, I., Hatté, C., Heaton, T.J., Hoffmann, D.L., Hogg, A.G., Hughen, K.A., Kaiser, K.F.,
665 Kromer, B., Manning, S.W., Niu, M., Reimer, R.W., Richards, D.A., Scott, M.E., Southon, J.R.,
666 Turney, C.S.M., and van der Plicht, J.: IntCal13 and Marine13 radiocarbon age calibration
667 curves 0-50,000 yr cal BP, *Radiocarbon*, 55, 4, 1869-1887, 2013.

668 **Robertson, A. W., and Mechoso, C. R.: Interannual and interdecadal variability of the**
669 **South Atlantic Convergence Zone. *Mon. Wea. Rev.*, 128, 2947-2957, 2000.**

670 Romero, O. E., Lange, C. B., Fischer, G., Treppke, U. F., and Wefer, G.: Variability in
671 export production documented by downward fluxes and species composition of marine planktonic
672 diatoms: Observations from the tropical and equatorial Atlantic, in: *Use of proxies in*
673 *paleoceanography: Examples from the South Atlantic*, edited by: Fischer, G. and Wefer, G.,
674 Universitat Bremen, Springer, Germany, 365–392, 1999.

675 Salazar, A., Lizano, O. G. and Alfaro, E. J.: Composición de sedimentos en las zonas
676 costeras de Costa Rica utilizando Fluorescencia de Rayos-X (FRX), *Rev. biol. Trop.*, 52, 2,
677 2004.

678 Salvattecí, R., Gutiérrez, D., Field, D. and Sifeddine, D., Ortlieb, L., Bouloubassi, I.,
679 Boussafir, M., Boucher, H and Cetin, F.: The response of the Peruvian Upwelling Ecosystem to
680 centennial-scale global change during the last two millennia, *Clim. Past*, 10, 715–731,
681 doi:10.5194/cp-10-715-2014, 2014.

682 Sar, E. A., Sunesen, I. and Lavigne, A. S.: *Cymatotheca*, *Tryblioptychus*, *Skeletonema*
683 and *Cyclotella* (Thalassiosirales) from Argentinian coastal waters. Description of *Cyclotella*
684 *cubiculata* sp. nov., *Vie milieu*, 60, 2, 135-156, 2010.

685 Sifeddine, A., Gutiérrez, D., Ortlieb, L., Boucher, H., Velazco, F., Field, D., Vargas, G.,
686 Boussafir, M., Salvattecí, R., Ferreira, V., García, M., Valdés, J., Caquineau, S., Mandeng
687 Yogo, M., Cetin, F., Solis, J., Soler, P. and Baumgartner, T.: Laminated sediments from the
688 central Peruvian continental slope: A 500 year record of upwelling system productivity,
689 terrestrial runoff and redox conditions, *Prog. Oceanog.*, 79, 2-4, 190-197, 2008.

690 **Strikis, N. M., Cruz Jr., F. W., Cheng, H., Karmann, I., Edwards, R. L., Vuille, M.,**
691 **Wang, X., de Paula, M. S., Novello, V. F., and Auler, A. S.: Abrupt variations in South**

692 American monsoon rainfall during the Holocene based on a speleothem record from central-
693 eastern Brazil, *Geology*, 39, 1075–1078, 2011.

694 Urien, C. M., and Ewing, M.: Recent sediments and environment of southern Brazil,
695 Uruguay, Buenos Aires, and Rio Negro continental shelf, in: *The Geology of Continental*
696 *Margins*, edited by: Burk, C. A., and Drake, C. L., Springer, New York, 157-177, 1974.

697 Urien, C. M., Martins, L. R., and Martins, I. R.: Evolução geológica do Quaternário do
698 litoral atlântico uruguaio, plataforma continental e regiões vizinhas, *Notas Técnicas*,
699 *CECO/URFGS*, 3, 7-43, 1980.

700 Vázquez-Castro, G., Ortega-Guerrero, B., Rodríguez, A., Caballero, M., and Lozano-
701 García, S.: Mineralogía magnética como indicador de sequía en los sedimentos lacustres de los
702 últimos *ca.* 2,600 años de Santa María del Oro, occidente de México, *Rev. Mex. Cienc. Geol.*,
703 25, 1, 21-38, 2008.

704 Vuille, M., Burns, S. J., Taylor, B. L., Cruz, F. W., Bird, B.W., Abbott, M. B., Kanner, L.
705 C., Cheng, H., and Novello V. F.: A review of the South American monsoon history as recorded
706 in stable isotopic proxies over the past two millennia, *Clim. Past.*, 8, 1309–1321, doi:10.5194/cp-
707 8-1309-2012, 2012.

708 Weltje, G. J., and Tjallingii, R.: Calibration of XRF core scanners for quantitative
709 geochemical logging of sediment cores: Theory and application, *Earth Planet. Sci. Lett.*, 274, 3–
710 4, 423–438. doi:10.1016/j.epsl.2008.07.054, 2008.

711 Witkowski, A., Lange-Bertalot, H., and Metzeltin, D.: Diatom flora of marine coasts 1,
712 in: *Iconographia Diatomologica*, edited by: Lange-Bertalot, H., and Gantner Verlag A.R.G., 7,
713 925, 2000.

714 Yarincik, K., Murray, M., R. W., and Peterson, L. C: Climatically sensitive eolian and
715 hemipelagic deposition in the Cariaco Basin, Venezuela, over the past 578,000 years: Results
716 from Al/Ti and K/Al, *Paleoceanography*, 15, 2, 210–228, doi:10.1029/1999PA900048, 2000.

717 Zhou, J. and Lau, K.-M.: Does a monsoon climate exist over South America?, *J. Climate*,
718 11, 1020–1040, 1998.

719

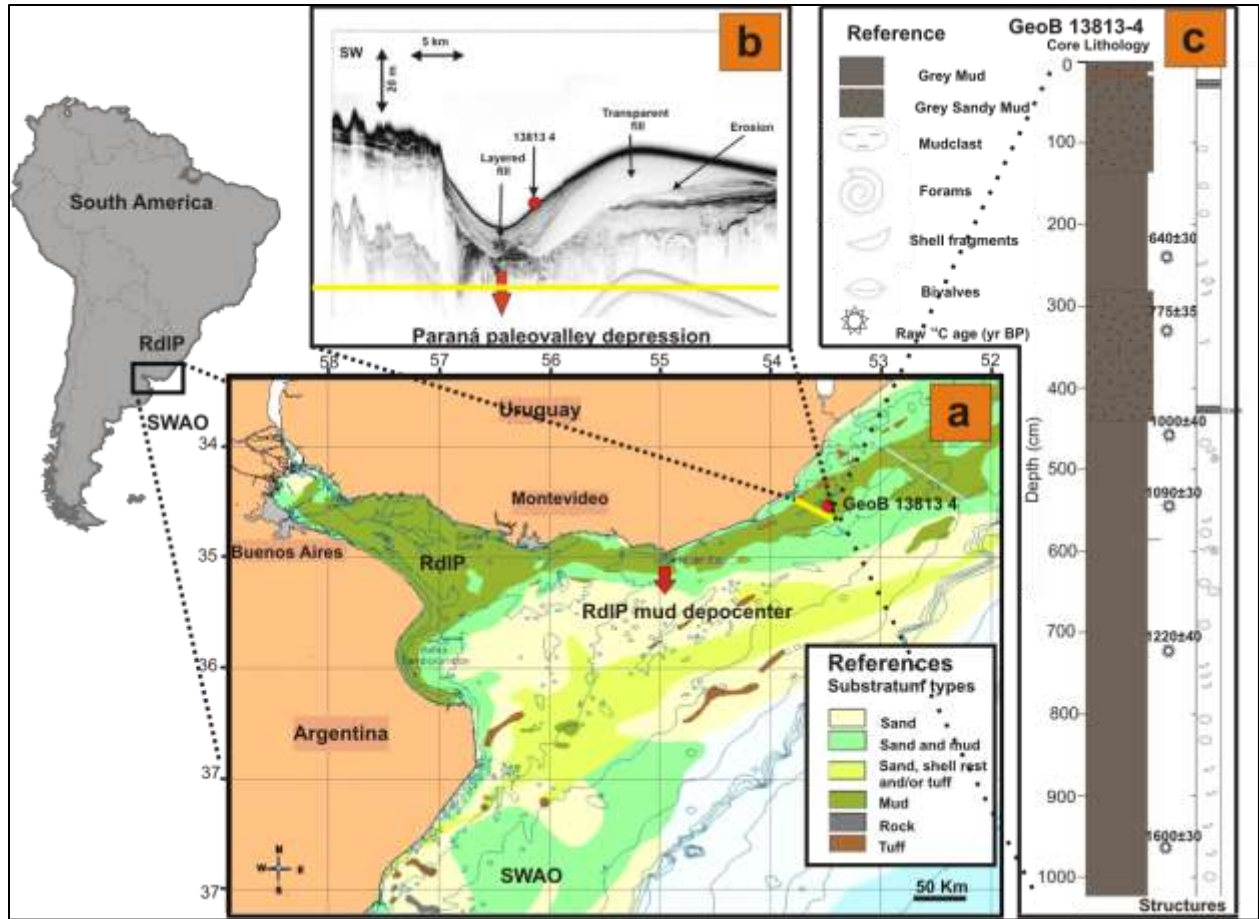
720

Table 1. Radiocarbon dates as obtained from the Bacon modeling.

Lab # (Poz-)	Depth in core (cm)	Raw ¹⁴C age (yr BP)	Bacon weighted average age (cal yr BP)	Bacon weighted average age (cal yr AD)	Sedimentation rate (cm yr⁻¹)
35198	255	640± 30	230	1688	0.72
47935	305	775± 35	371	1494	0.68
42428	447	1000± 40	552	1293	0.78
35199	560	1090± 30	665	1167	1.00
47937	705	1220± 40	830	994	0.88
42429	964	1600± 30	1197	753	0.70

721

722



723

724 **Fig.1. (a)** Study area: The red circle indicates the location of Core GeoB 13813-4 retrieved from
 725 the inner-shelf mud depocenter off the Uruguayan coast (modified from Freplata, 2004). **(b)** Rio
 726 de la Plata (RdIP) mud depocenter (PARASOUND sub-bottom profile), which represents the RdIP
 727 paleo-valley and its sedimentary multi-story filling succession. **(c)** GeoB 13813-4 core lithology.
 728 (1b and 1c modified from Krastel et al., 2012 and Lantzsch et al., 2014). Stars on the right of the
 729 sediment core indicate ¹⁴C-dated intervals.

730

731

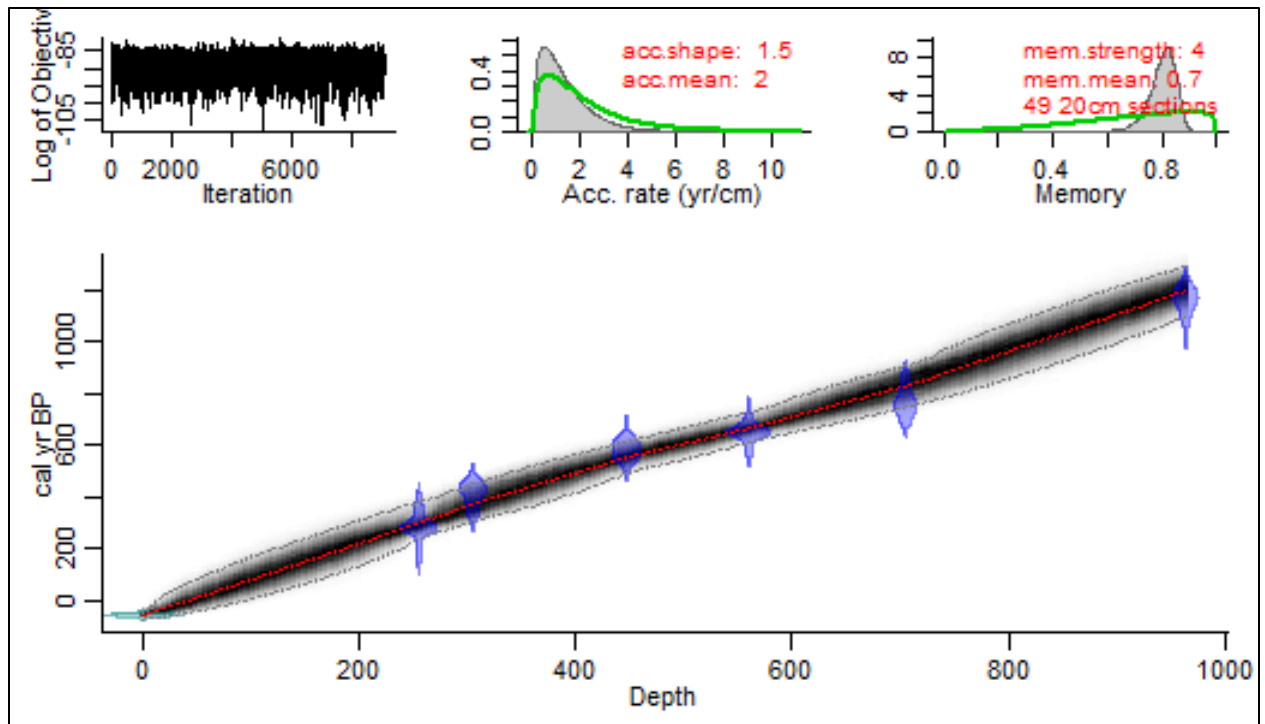
732

733

734

735

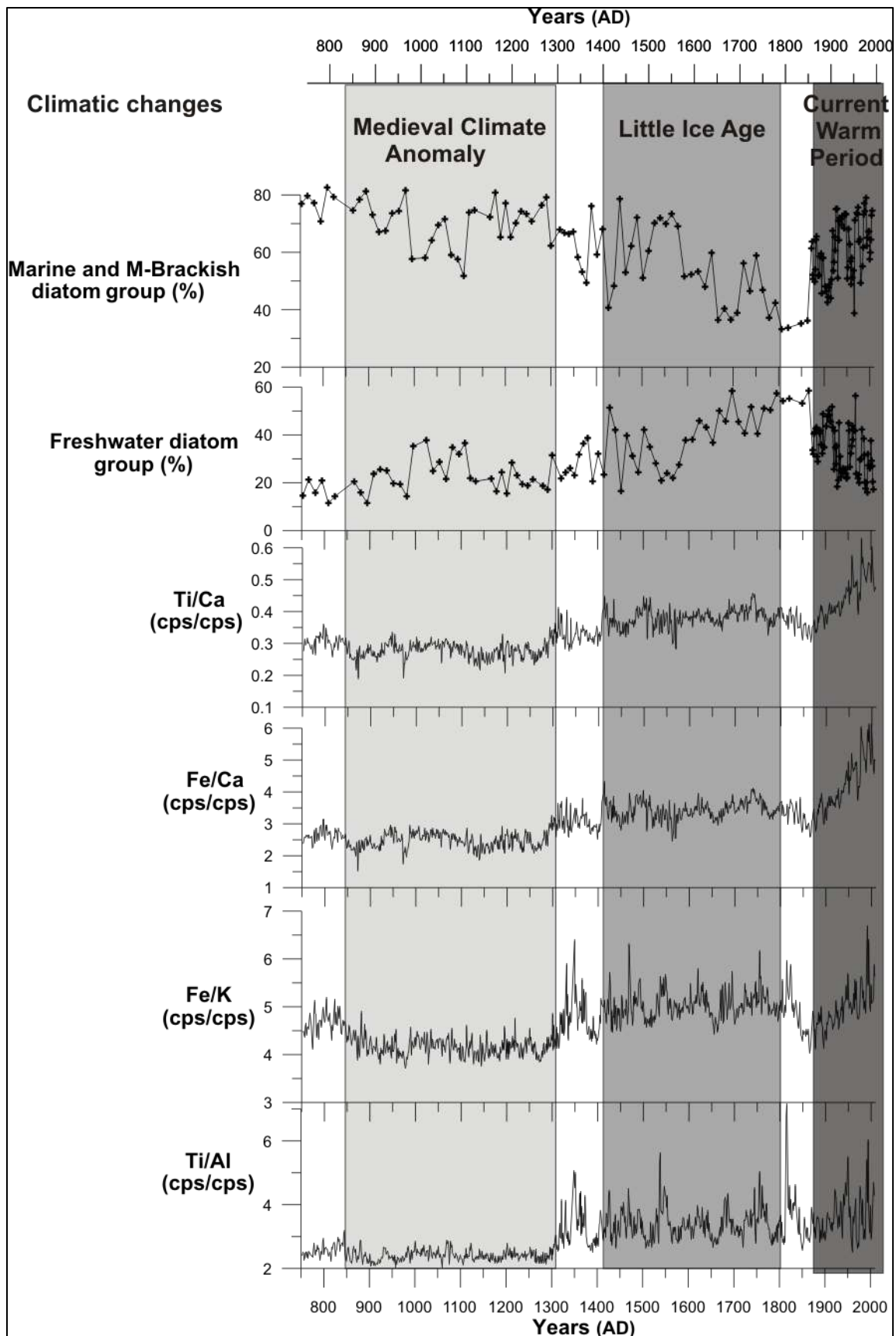
736



737

738 **Fig. 2.** The age-depth model for core GeoB 13813-4 using the program Bacon. Upper panels
 739 depict the Markov Chain Monte Carlo (MCMC) iterations (left), the prior (green curves) and
 740 posterior (grey histograms) distributions for the sedimentation rate (middle panel) and memory
 741 (right panel). The bottom panel shows the calibrated ^{14}C dates (transparent blue), extraction year
 742 of the core (-59 yr BP, 2009 AD, transparent blue light) and the age-depth model (grey stippled
 743 lines indicate the 95 % confidence intervals; the red curve shows the 'best' fit based on the
 744 weighted mean age for each depth).

745



747 **Fig. 3.** Centennial variation of Ti/Al, Fe/K, Ti/Ca, Fe/Ca ratios, and the freshwater and marine,
748 marine-brackish salinity-indicative diatom groups from the sediment core GeoB 13813-4 (from
749 bottom to top, respectively), during the last 1200 yr BP (750-2000 cal yr AD). The major
750 climatic changes during this period of time were the Medieval Climatic Anomaly and the Little
751 Ice Age.

752